



## OPEN

SUBJECT AREAS:  
MESOTHELIOMA  
CANCERReceived  
12 February 2014Accepted  
4 August 2014Published  
21 August 2014Correspondence and  
requests for materials  
should be addressed to  
A.L.H. (amanda.  
hudson@sydney.edu.  
au)

# Establishing a panel of chemo-resistant mesothelioma models for investigating chemo-resistance and identifying new treatments for mesothelioma

Amanda L. Hudson<sup>1,2</sup>, Chris Weir<sup>1,2</sup>, Elizabeth Moon<sup>1,2</sup>, Rozelle Harvie<sup>1,2</sup>, Sonja Klebe<sup>3</sup>,  
Stephen J. Clarke<sup>1,2</sup>, Nick Pavlakis<sup>1,2</sup> & Viive M. Howell<sup>1,2</sup>

<sup>1</sup>Bill Walsh Translational Cancer Research Laboratory, Kolling Institute of Medical Research, University of Sydney, Royal North Shore Hospital, St. Leonards, New South Wales, Australia, <sup>2</sup>Department of Medical Oncology, Royal North Shore Hospital, University of Sydney, St. Leonards, New South Wales, Australia, <sup>3</sup>Department of Anatomical Pathology, Flinders University and SA Pathology, Adelaide, Australia.

Mesothelioma is inherently chemo-resistant with only 50% of patients responding to the standard of care treatments, and consequently it has a very grim prognosis. The aim of this study was to establish a panel of chemo-resistant mesothelioma models with clinically relevant levels of resistance as tools for investigating chemo-resistance and identifying new treatments for mesothelioma. Chemo-resistant cell lines were established *in vitro* and characterized *in vivo* using syngeneic Fischer rats. Tumors derived from all chemo-resistant cell lines were immunohistochemically classified as mesothelioma. Homozygous deletion of p16<sup>INK4A</sup>/p14<sup>ARF</sup> and increased expression of several *ATP-binding cassette* transporters were demonstrated, consistent with findings in human mesothelioma. Further, the acquisition of chemo-resistance *in vitro* resulted in changes to tumor morphology and overall survival. In conclusion, these models display many features corresponding with the human disease, and provide the first series of matched parental and chemo-resistant models for *in vitro* and *in vivo* mesothelioma studies.

Malignant mesothelioma (MM) is an aggressive malignancy that displays relatively low responses to existing therapies resulting in short survival for those afflicted. Exposure to asbestos fibres is known in 80% of all MM patients with an estimated 125 million people exposed globally in the workplace leading to 43,000 people dying of MM each year (reviewed in<sup>1</sup>). While bans on asbestos use were introduced decades ago in most western countries, its widespread use means that existing asbestos in the community remains a real danger to the general public<sup>2,3</sup>. This together with the long latency period for tumor development means that MM incidence continues to increase, with a new incidence wave emerging due to non-occupational exposure, and there is uncertainty as to when, and at what level it will peak<sup>3</sup>.

The most effective chemotherapy was established in 2003 and combines the use of pemetrexed and cisplatin<sup>4</sup>; this remains the current standard of care<sup>5</sup>. Whilst MM is inherently chemo-resistant, approximately 40% of patients will respond to this treatment<sup>6</sup> leading to a median survival of 12 months<sup>7</sup>. Thus there is an urgent need to identify more effective treatments for mesothelioma patients. While a number of novel therapies have recently been examined in clinical trials<sup>8</sup>, to date none of these has resulted in changes in practice. This is due in part to a general lack of successful translation of promising pre-clinical data to the clinical setting in cancer, with only 5% of drugs entering clinical trials ultimately approved by the Food and Drug Administration<sup>9,10</sup>. A significant contributor to this high failure rate is the lack of 'robustness' of the pre-clinical models used to evaluate new treatments<sup>11</sup>. The majority of pre-clinical assessments for candidate therapeutics are performed *in vitro* and in xenograft mouse models<sup>12</sup>. These do not always recapitulate the cellular complexity of clinical tumors<sup>10</sup>, occurring in non-physiological environments, frequently in the absence of both immune surveillance and systemic interactions with the vascular system<sup>13</sup>. While no model is ideal, syngeneic orthotopic models have the advantage of representing the dynamics of the complete tumor by allowing essential interactions between tumor cell receptors,

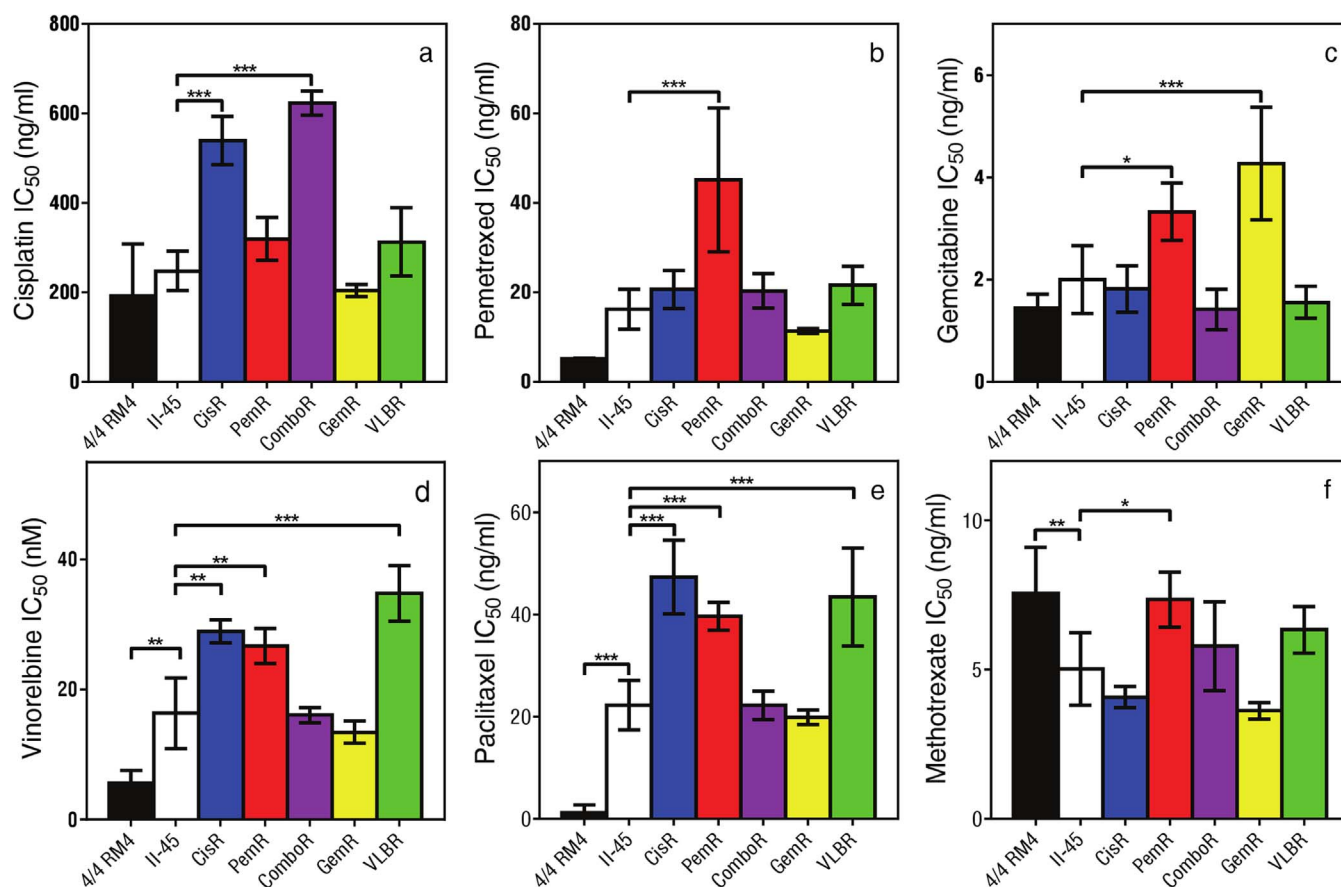


**Figure 1** | IC<sub>50</sub> values for cell lines. Cell viability of the mesothelial, parental and chemo-resistant mesothelioma cells were assessed using MTT assays in the presence of therapeutic agent as indicated. The drug dose causing 50% growth inhibition (IC<sub>50</sub> drug dose) was calculated. While the 4/4 RM.4 cells grew significantly slower than the II-45 cells ( $p < 0.05$ ) with doubling times of  $18.1 \pm 0.9$  hrs and  $14.5 \pm 0.9$  hrs respectively, the percentage survival for the cytotoxicity assays is based on the growth of each individual cell line grown without the addition of chemotherapeutic agent and is thus independent of differences in growth rates between the cell lines. Bars show the mean and the error bars show the standard error from at least three independent experiments. P-value was calculated using a one-way Anova test with a value of less than 0.05 indicating significance. \* $p < 0.05$ , \*\* $p < 0.01$ , \*\*\* $p < 0.001$  relative to parental II-45 mesothelioma cells. Mesothelial cells, 4/4 RM.4, parental mesothelioma cells, II-45; cisplatin resistant II-45 cells, CisR; pemetrexed resistant II-45 cells, PemR; combination (cisplatin + pemetrexed) resistant II-45 cells, ComboR; gemcitabine resistant II-45 cells, GemR; vinorelbine resistant II-45 cells, VLBR.

the stromal ligands and a functioning immune system creating a more realistic environment for tumor development<sup>14</sup>.

Since its development in 1987<sup>15</sup>, the syngeneic II-45 rat mesothelioma cell line, also referred to as IL-45<sup>16</sup>, has been accepted and utilized as a relevant model system for pleural mesothelioma research<sup>17–20</sup>. This model exhibits an essentially sarcomatoid morphology<sup>16</sup>. While sarcomatoid mesothelioma accounts for only 10–15% of all diagnosed cases, it is more aggressive and less responsive to treatment<sup>21</sup> resulting in decreased survival<sup>22</sup>. Using the least responsive subtype as a model may help to identify new treatments which are effective for the other subtypes as well. However, given the high likelihood of acquiring chemo-resistance, models which have acquired clinically relevant levels of resistance are also needed. This paper establishes and characterizes a panel of chemo-resistant mesothelioma models with clinically relevant levels of resistance and investigates their phenotypic differences. Such models that recapitulate human disease, will not only enable mechanistic studies into the causes of chemo-resistance, but will also facilitate the identification of new treatments.

## Results

**Normal mesothelial and II-45 mesothelioma cells have different drug sensitivity profiles.** Given the inherent chemo-resistance of

MM, we first wanted to determine whether the chemo-naïve II-45 mesothelioma cell line had different chemotherapeutic responses to those of normal strain-matched mesothelial cells (4/4 RM.4 cells). 4/4 RM.4 cells were chosen as they represent the ‘putative progenitor cells’ of MM and as such an accepted non-malignant control for the II-45 cells<sup>23–25</sup>. Using MTT cytotoxicity assays, we observed that the II-45 cells were 20-fold more resistant to paclitaxel ( $p < 0.001$ ) and 3-fold more resistant to vinorelbine ( $p < 0.01$ ) than the non-malignant control cells, confirming the inherent resistance of the II-45 cells to these anti-mitotic agents (Figure 1). A trend towards increased resistance was observed for pemetrexed. However, these cells were not inherently resistant to all agents assessed, showing equivalent sensitivities to the non-malignant cells for cisplatin and gemcitabine, and increased sensitivity to methotrexate (Figure 1).

**Establishment of 5 chemo-resistant mesothelioma cell lines *in vitro*.** To be able to address the critical clinical issue of resistance to chemotherapy we sought to establish mesothelioma cell models with acquired resistance to the standard of care and other agents used for the treatment of MM. Clinically, dose escalation in patients is generally not feasible due to the associated increase in toxicity with the recommended dosage being based on the maximum tolerated dose. To recapitulate this clinical scenario, the drug concentration used to generate chemo-resistance cells in this study remained



Table 1 | Significant changes in gene expression levels in II-45 mesothelioma cells in relation to normal 4/4 RM.4 mesothelial cells

Gene name	Abbreviation	Functional gene grouping	Fold change
ATP-binding cassette, sub-family B (MDR/TAP), member 1A	<i>Abcb1a</i> *	Drug resistance	243.9 <sup>A</sup>
ATP-binding cassette, subfamily G (WHITE), member 2	<i>Abcg2</i>	Drug resistance	26.1
Major vault protein	<i>Mvp</i>	Drug resistance	6.5
Tumor protein p53	<i>Tp53</i>	Drug resistance	2.3
Cellular retinoic acid binding protein 1	<i>Crabp1</i>	Drug metabolism	9.4 <sup>A</sup>
Cytochrome P450, family 2, subfamily b, polypeptide 2	<i>Cyp2b2</i>	Drug metabolism	5.5 <sup>A</sup>
Cytochrome P450, subfamily 2, polypeptide 11	<i>Cyp2c11</i>	Drug metabolism	-15.4 <sup>A</sup>
Dihydrofolate reductase	<i>Dhfr</i>	Drug metabolism	1.9
Epoxide hydrolase 1, microsomal	<i>Ephx1</i>	Drug metabolism	-44.5
Glutathione S-transferase mu 1	<i>Gstm1</i>	Drug metabolism	2.6
Superoxide dismutase 1, soluble	<i>Sod1</i>	Drug metabolism	2.3
UDP-glucose ceramide glucosyltransferase	<i>Ugcg</i>	Drug metabolism	9.0
Cyclin D1	<i>Ccnd1</i>	Cell cycle	5.3
Cyclin dependent kinase 2	<i>Cdk2</i>	Cell cycle	1.5
Cyclin-dependent kinase inhibitor 1B	<i>Cdkn1b</i>	Cell cycle	-2.5 <sup>A</sup>
Similar to cyclin-dependent kinase inhibitor 2D	<i>Cdkn2d</i>	Cell cycle	2.3
Epidermal growth factor receptor	<i>Egfr</i>	Growth factor receptor	-9.8
Fibroblast growth factor 2	<i>Fgf2</i>	Growth factor receptor	19.7 <sup>A</sup>
Met proto-oncogene	<i>Met</i>	Growth factor receptor	-2.7
Androgen receptor	<i>Ar</i> *	Hormone receptor	215.7 <sup>A</sup>
Peroxisome proliferator-activated receptor delta	<i>Ppard</i>	Hormone receptor	2.8
Peroxisome proliferator-activated receptor gamma	<i>Pparg</i>	Hormone receptor	65.4 <sup>A</sup>
Aryl hydrocarbon receptor	<i>Ahr</i>	Transcription factor	-21.5
Adaptor-related protein complex 1, sigma 1 subunit	<i>Ap1s1</i>	Transcription factor	8.5
Myelocytomatosis oncogene	<i>Myc</i>	Transcription factor	5.4
Nuclear factor of kappa light polypeptide gene enhancer in B-cells inhibitor, beta	<i>Nfkbib</i>	Transcription factor	2.2
ATP-binding cassette, sub-family B (MDR/TAP), member 1A	<i>Abcb1a</i>	Drug resistance	153.7
Androgen receptor	<i>Ar</i>	Hormone receptor	235.0

\*Validated using individual TaqMan Gene Expression Assays; results normalized to Rplp1, Actb and Gapdh.

<sup>A</sup>Assay reached detection limit therefore result not accurate and likely to be higher than indicated. Results generated by rat SABioscience PCR arrays using SYBR green (Qiagen); results normalized to a panel of housekeeping genes (Rplp1, Hprt1, Rpl13a, Ldha, Actb) and are the mean of three biological replicates.

constant. Chemo-resistant cell lines were generated by treating the parental II-45 cells with the drug concentration required for 50% growth inhibition (IC<sub>50</sub>) for each drug followed by a recovery period. In addition to dosing with cisplatin, pemetrexed, gemcitabine or vinorelbine individually, the combination treatment of cisplatin plus pemetrexed, as the current standard of care regimen, was also included (ComboR). After 15 cycles of drug treatment the resulting cell lines developed clinically<sup>26</sup> and statistically significant increases in resistance to the chemotherapeutic agent they were selected against (Figure 1,  $p < 0.05$  relative to parental II-45 cells). There were no significant differences seen in growth rates between the parental and chemo-resistant II-45 cells *in vitro* (data not shown).

Interestingly, cross resistance to other classes of anti-cancer agents was observed indicating potential multi-resistant phenotypes (Figure 1). Cells with acquired resistance to pemetrexed (PemR) demonstrated the broadest cross-resistance, having developed resistance to gemcitabine, vinorelbine, paclitaxel and methotrexate, but maintaining sensitivity to cisplatin. Cells with acquired resistance to cisplatin (CisR) were also observed to be resistant to the anti-mitotics vinorelbine and paclitaxel.

**II-45 cells have high endogenous expression of drug resistance-related genes.** In order to utilise the cell models developed above for overcoming chemo-resistance we were interested in identifying mechanisms of resistance in common with the human malignancy. We surveyed the expression of a focussed panel of 84 genes involved in the response to chemotherapy that had previously been shown to have relevance to human mesothelioma<sup>(27, SI Table 1 for a list of the gene panel)</sup>. Consistent with changes reported for human MM cell lines and tissues, large changes were seen in the ATP-binding cassette (ABC) transporter superfamily members involved in drug resis-

tance<sup>28</sup>. *Abcb1a* and *Abcg2* were vastly elevated in parental II-45 cells relative to the non-malignant control cells (Table 1). These vast increases in transcript levels were maintained or increased further in the 5 chemo-resistant cell lines (Table 2, results expressed relative to II-45 parental cells). Changes in expression of *Abcb4*, *Abcc2* and, or *Abcg2* were also noted between the chemo-resistant and parental II-45 cell lines with vinorelbine resistant cells (VLBR) demonstrating increased expression of all 3 genes (Table 2).

Large changes in expression between the malignant and non-malignant control cells were observed for a number of other genes in the selected panel assessed (Table 1). Notable were the hormone receptors *Androgen receptor (Ar)* and *Peroxisome proliferator-activated receptor gamma (Pparg)* which were also found to be amongst the top 10 most upregulated genes in human MM cell lines relative to non-malignant control cells<sup>27</sup>. The expression levels of these genes had been shown to be altered by the mitogen-activated protein kinase kinase 1 (MEK1) inhibitor U0126 suggesting a role for mitogen-activated protein kinase 3 (MAPK3 or ERK1) in their regulation<sup>27</sup>. We also found that the expression of *Ar* varied significantly with the resistance profile of the cells with a decrease in expression observed for cells resistant to pemetrexed and/or cisplatin (Table 2).

To further understand the resistance mechanisms that may be used by the newly established II-45 chemo-resistant cell lines we undertook additional gene expression analysis (Taqman assays) for several key genes. Transcript levels of *excision repair cross complementation group 1 (Ercc1)*<sup>29</sup>, *ribonucleotide reductase M1 (Rrm1)*<sup>30</sup> and *thymidylate synthetase (Tyms)*<sup>31</sup> are known to correlate with cisplatin, gemcitabine or pemetrexed resistance respectively. However, no significant differences in the expression of these genes were observed between the cell lines (supplementary Figure 1) indicating that these genes do not have major roles in the mechanisms responsible for chemo-resistance in these cell lines.

Table 2 | Significant gene expression changes ( $p < 0.05$ ) in chemo-resistant II-45 cells in relation to parental II-45 cells

Gene Abbreviation	Functional gene grouping	CisR	PemR	ComboR	GemR	VLBR
<i>Abcb1a</i> *	Drug resistance	1.6	-	-	-	1.9
<i>Abcb1b</i> *	Drug resistance	1.6	-	-	-	-
<i>Abcb4</i>	Drug resistance	-	-2.2	-	-2.6	2.8
<i>Abcc2</i>	Drug resistance	-	2.0	1.6	-	2.1
<i>Abcg2</i>	Drug resistance	-	-	-	-	2.4
<i>Bcl2</i>	Drug resistance	-	-	1.3	-	-
<i>Bcl2l1</i>	Drug resistance	-	2.0	-	-	-
<i>Rb1</i>	Drug resistance	-	-	-1.8	-	-
<i>Crabp1</i>	Drug metabolism	6.8	-	2.3	-	-
<i>Cyp2b2</i>	Drug metabolism	-	-	2.2	-	9.5
<i>Cyp2c7</i>	Drug metabolism	-	-	3.9	-	-
<i>Dhfr</i>	Drug metabolism	-	-	1.3	-	-
<i>Ephx1</i>	Drug metabolism	-	-	-5.5	-	-
<i>Nat2</i>	Drug metabolism	-1.7	-	-1.7	-	-
<i>Sod1</i>	Drug metabolism	1.3	-	1.2	-	-
<i>Ugcg</i>	Drug metabolism	-	-	-	-	-1.6
<i>Xpa</i>	DNA repair	-	-1.2	-1.8	-	-
<i>Ccnd1</i>	Cell cycle	1.5	1.1	-	-	-
<i>Cdkn1a</i>	Cell cycle	-	-	-1.8	-	-
<i>Fgf2</i>	Growth factor receptor	-	-	-2.3	-	-
<i>Ar</i> *	Hormone receptor	-7.7 <sup>A</sup>	-36.8 <sup>A</sup>	-72.1 <sup>A</sup>	2.8	-
<i>Ppard</i>	Hormone receptor	-2.3	-	-	-	-
<i>Pparg</i>	Hormone receptor	-	-	-2.4	-2.1	-
<i>Gabpa</i>	Transcription factor	1.8	-	-	-	1.7
<i>Myc</i>	Transcription factor	-	1.6	-	-	-
<i>Abcb1a</i>	Drug resistance	1.44	-	-	-	1.21
<i>Abcb1b</i>	Drug resistance	1.40	-	-	-	-
<i>Ar</i>	Hormone receptor	-7.35	-33.30	-49.02	3.23	-

\*Validated using individual TaqMan Gene Expression Assays; results normalized to Rplp1, Actb and Gapdh.

<sup>A</sup>Assay reached detection limit therefore the result is likely to be higher than indicated. - indicates result was not significantly different ( $p \geq 0.05$ ). II-45, parental mesothelioma cells; CisR, cisplatin resistant II-45 cells; PemR, pemetrexed resistant II-45 cells; ComboR, combination (cisplatin + pemetrexed) resistant II-45 cells; GemR, gemcitabine resistant II-45 cells; VLBR, vinorelbine resistant II-45 cells. Results generated by rat SABioscience PCR arrays using SYBR green (Qiagen); results normalized to a panel of housekeeping genes (Rplp1, Hprt1, Rpl13a, Ldha, Actb, Rplp1) and are the mean of three biological replicates.

**ABC transporter superfamily members are associated with inherent and acquired drug resistance in II-45 mesothelioma cell lines.** Given the vast expression changes noted in several ABC transporter genes we next sought to functionally confirm the contribution of the ABC transporter proteins to the resistance profiles of the cell lines. Pemetrexed and vinorelbine are known substrates of the ABC transporters<sup>32</sup>. Parental II-45 cells and cells with acquired resistance to pemetrexed (PemR) or vinorelbine (VLBR) were treated with the drug in the presence or absence of verapamil, an ABC transporter protein inhibitor, and their sensitivities ( $IC_{50}$ ) reassessed. In the presence of verapamil, the ABC transporter efflux of drug is inhibited and the sensitivity of VLBR cells to vinorelbine, and PemR cells to pemetrexed increased significantly (Figure 2C and D,  $p < 0.05$  and  $p < 0.01$ , respectively). These results confirm the contribution of the ABC transporter proteins in resistance to pemetrexed and vinorelbine.

**Glutathione levels are not responsible for cisplatin resistance in II-45 cell lines.** We similarly attempted to understand the mechanisms involved in resistance to cisplatin. Increased glutathione (GSH) levels have been documented to correlate with cisplatin resistance<sup>33</sup>. Therefore we treated parental II-45 and cisplatin resistant cell lines (CisR and ComboR) with cisplatin with and without an inhibitor of GSH and reassessed the sensitivities to cisplatin. The addition of the GSH inhibitor, buthionine sulfoximine (BSO), led to a decrease in the resistance of the CisR and ComboR cell lines to cisplatin (supplementary Figure 2). However, these results did not reach significance indicating that increased GSH levels are not the major mechanism for cisplatin resistance in these models. This is similarly reflected in the increased expression of the GSH conjugating enzyme transcript

*Gstm1* in the II-45 cells (Table 1, relative to non-malignant cells) which was insufficient to alter cisplatin sensitivity (Figure 1A).

**Comparative genomic hybridization identifies loss of the *Cdkn2* locus in II-45 cells.** The most common chromosomal change in human MM is homozygous deletion of the  $p16^{INK4A}/p14^{ARF}$  locus which occurs in 50–70% of human mesothelioma samples and in up to 90% of stable MM cell lines<sup>34</sup>. To determine whether this genetic aberration is also present in our models, comparative genomic hybridization (CGH) arrays were performed on selected cells lines (II-45 parental and ComboR). Of the chemo-resistant cell lines established, the ComboR cells were chosen as they were treated simultaneously with two different drugs (cisplatin and pemetrexed) which would put them under more selective pressure than the other cell lines. Homozygous deletion of *Cdkn2a/2b* along with a co-deletion of *Mtap* at 5q32 was identified in both the parental and combination resistant II-45 cells (supplementary Figure 3) providing chromosomal evidence for the relevance of these models to the human malignancy. Complete (homozygous) loss of *Cdkn2* was also noted by gene expression profiling with no transcript expression detected (data not shown). Alterations at *Nf2*, *Tp53*, *Bap1* or *Egfr* are also noted in subsets of MM cases. However, no chromosomal abnormalities were identified at these loci in the II-45 cell lines.

**Rats engrafted with pemetrexed resistant cells have a shorter survival than those engrafted with parental chemo-naïve cells.** Having established the series of chemo-resistant cell lines and identified gene and chromosomal similarities with the human disease we next wished to determine whether there were *in vivo* differences in growth characteristics between these cell lines. Rats

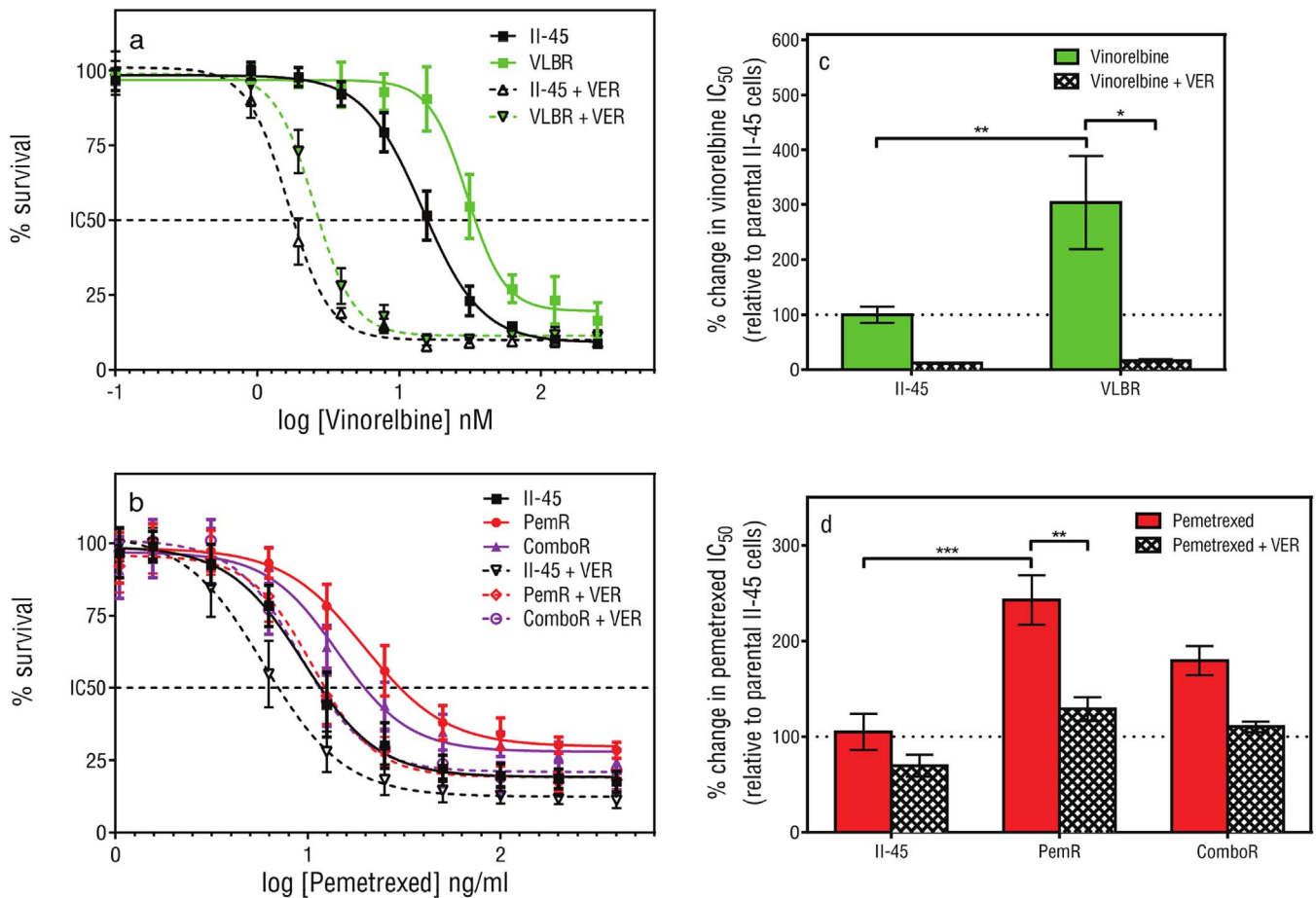


**Figure 2 | The effect of inhibiting ABC transporters on cell viability.** Cell viability of parental and chemo-resistant mesothelioma cells following vinorelbine (a, c) or pemetrexed (b, d) treatment in the presence (+VER) or absence of verapamil was determined using MTT assays. Points show the mean and standard error of triplicate wells. The drug dose causing 50% growth inhibition (IC<sub>50</sub> drug dose; c, d) was determined and the p-value was calculated by comparing the IC<sub>50</sub> values from at least three independent experiments using a one-way Anova test with a value of less than 0.05 indicating significance. \* $p < 0.05$ , \*\* $p < 0.01$ , \*\*\* $p < 0.001$ . Parental mesothelioma cells, II-45; pemetrexed resistant II-45 cells, PemR; combination (cisplatin + pemetrexed) resistant II-45 cells, ComboR; vinorelbine resistant II-45 cells, VLBR.

orthotopically engrafted with PemR cells reached ethically defined endpoints of euthanasia at day 11, significantly earlier than rats with parental II-45 cells ( $p < 0.05$ , Figure 3A). Overall the tumor scale in

the pleural cavity did not differ statistically between the groups (Figure 3B) although tumors from rats with PemR cells tended to be smaller.

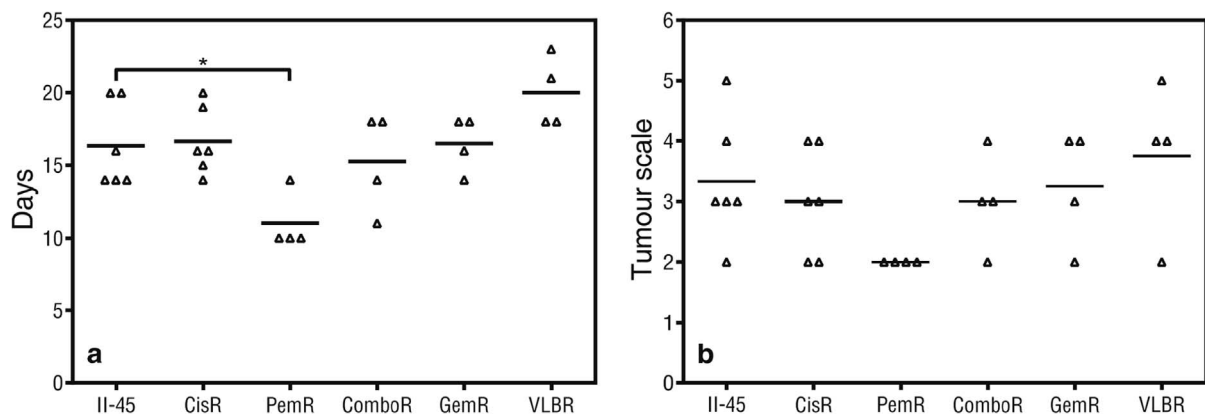


**Figure 3 | Endpoint data for rats with pleural mesothelioma.** Rats were injected with  $5 \times 10^5$  parental or chemo-resistant II-45 cells directly into the pleural cavity. (a) Mean time (days) until ethical endpoint (weight loss of  $>10\%$  or difficulty in breathing); (b) Pleural tumor scale at endpoint in rats with mesothelioma. P-value was calculated using a one-way Anova test with a value of less than 0.05 indicating significance. \* $p < 0.05$  relative to rats with II-45 mesothelioma cells. Parental mesothelioma cells, II-45; cisplatin resistant II-45 cells, CisR; pemetrexed resistant II-45 cells, PemR; combination (cisplatin + pemetrexed) resistant II-45 cells, ComboR; gemcitabine resistant II-45 cells, GemR; vinorelbine resistant II-45 cells, VLBR.

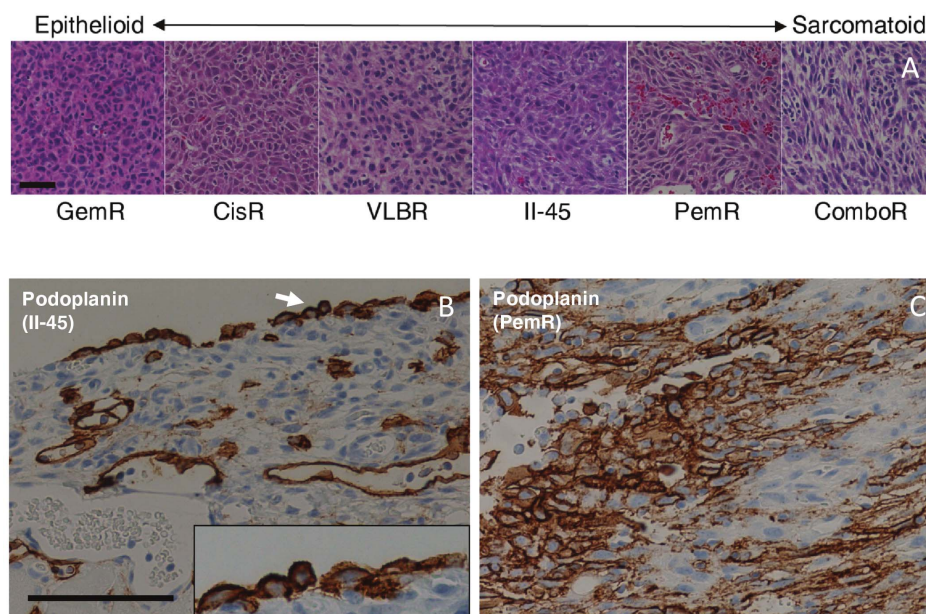


**Figure 4 | Histological images of pleural tumors derived from parental and chemo-resistant II-45 cells.** Representative images arranged according to morphological characteristics (a). Tumors with a distinctive epithelioid appearance are on the left ranging towards essentially sarcomatoid tumors on the right. GemR, gemcitabine resistant II-45 cells; CisR, cisplatin resistant II-45 cells; VLBR, vinorelbine resistant II-45 cells; II-45, parental mesothelioma cells; PemR, pemetrexed resistant II-45 cells; ComboR, combination (cisplatin + pemetrexed) resistant II-45 cells. Scale bar = 50  $\mu$ m. Podoplanin immunolabeling of tumors derived from parental (b) II-45 cells or pemetrexed resistant cells (c). Membranous immunolabeling of tumor cells and lymphatics (note lack of labelling of endothelial cells lining blood vessel) were identified in both tumor types with the labelling intensity increasing in the pemetrexed resistant tumors with labelling extending internally from the periphery. Inserts: 2 $\times$  higher magnification; Scale bar = 50  $\mu$ m.

**Chemo-resistance is maintained *in vivo*.** To confirm the maintenance of chemo-resistance *in vivo*, rats were engrafted with parental or CisR cells and then treated with cisplatin. Rats engrafted with CisR cells and subsequently treated with cisplatin survived for a substantially shorter period of time than rats engrafted with parental II-45 cells and similarly treated with cisplatin (Supplementary Figure 4A). *Ex-vivo* transplants were taken from tumors treated with cisplatin and grown under normal cell culture conditions. In comparison to II-45 tumor cells treated with cisplatin, CisR tumor cells treated with cisplatin were found to be statistically significantly resistant to cisplatin ( $p < 0.01$ ; supplementary Figure 4B&C) indicating that resistance is maintained *in vivo* when treated with chemotherapy.

**Tumor morphology changes with the acquisition of chemo-resistance.** The morphology of MM is classified as sarcomatoid, epithelioid or biphasic (a combination of both), with sarcomatoid morphology associated with poorer prognosis and reduced responsiveness to treatment<sup>21</sup>. We were therefore interested to determine whether the morphology had altered with the acquisition of chemo-resistance and performed H&E staining on at least 3 tumors from each cell line. We first established that the tumors arising from the parental chemo-naïve II-45 cells showed sarcomatoid morphology with pleomorphic features and only focal areas of epithelioid appearance (classified by pathologist S.K.) consistent with previous reports<sup>16</sup>. We next examined the tumors from the chemo-resistant cell lines and found that these demonstrated different morphologies ranging from epithelioid in the gemcitabine resistant tumors (GemR) to almost exclusively sarcomatoid in the PemR and ComboR tumors (Figure 4A). These distinct morphologies remained constant for each cell line across experiments ( $n \geq 3$ ) and were independent of the size and stage of the tumor. Significantly shorter survival correlated with a predominantly sarcomatoid morphology for the PemR rats (Figure 3a). However, no other associations between morphology and survival were observed.

The role of epithelial to mesenchymal transition (EMT) in the morphology of MM is uncertain<sup>35</sup>. Therefore, we assessed the levels of two well-known EMT markers E-cadherin and vimentin, as well as the proliferative marker Ki67 in the tumors. No differences in the levels of these proteins were detected by immunohistochemical (IHC) labelling between tumors with different morphologies (supplementary Figure 5). Proliferating Ki67 cells were found evenly throughout the sections and were not limited to the tumor periphery. These results indicated that EMT was not a major factor in the different morphologies observed and that the proliferative potential did not vary with morphology.

**Immunohistochemical characterization confirms a diagnosis of mesothelioma for all tumours and an increased sarcomatoid phenotype for PemR derived tumours.** In humans the diagnosis of MM can be difficult but is important for differentiation from reactive benign conditions and carcinomas. IHC analysis, performed in conjunction with histopathological examination is integral to the diagnosis and can assist with the classification of sarcomatoid or epithelioid subtypes. Having assessed tumor morphology and proliferative potential, we next examined the tumors using a diagnostic panel of antibodies recommended for the classification of human mesothelioma to determine whether the acquisition of chemo-resistance was accompanied by a change in IHC characteristics in addition to a change in morphology.

The human classification system recommends assessment of both positive and negative markers for MM. The positive markers include WT-1, HBME-1, calretinin, podoplanin and cytokeratins (5/6 and pan-cytokeratins using clone MMF116) with increased expression of calretinin indicative of an epithelioid subtype and increased expression of podoplanin indicative of a sarcomatoid subtype (detailed in SI Table 2). Recommended negative markers to differentiate MM from carcinomas include CD15 and TTF-1 (SI Table 2).

Using this antibody panel all tumors were diagnosed as mesothelioma ( $n = 3$  per cell line). All tumors were negative for the two

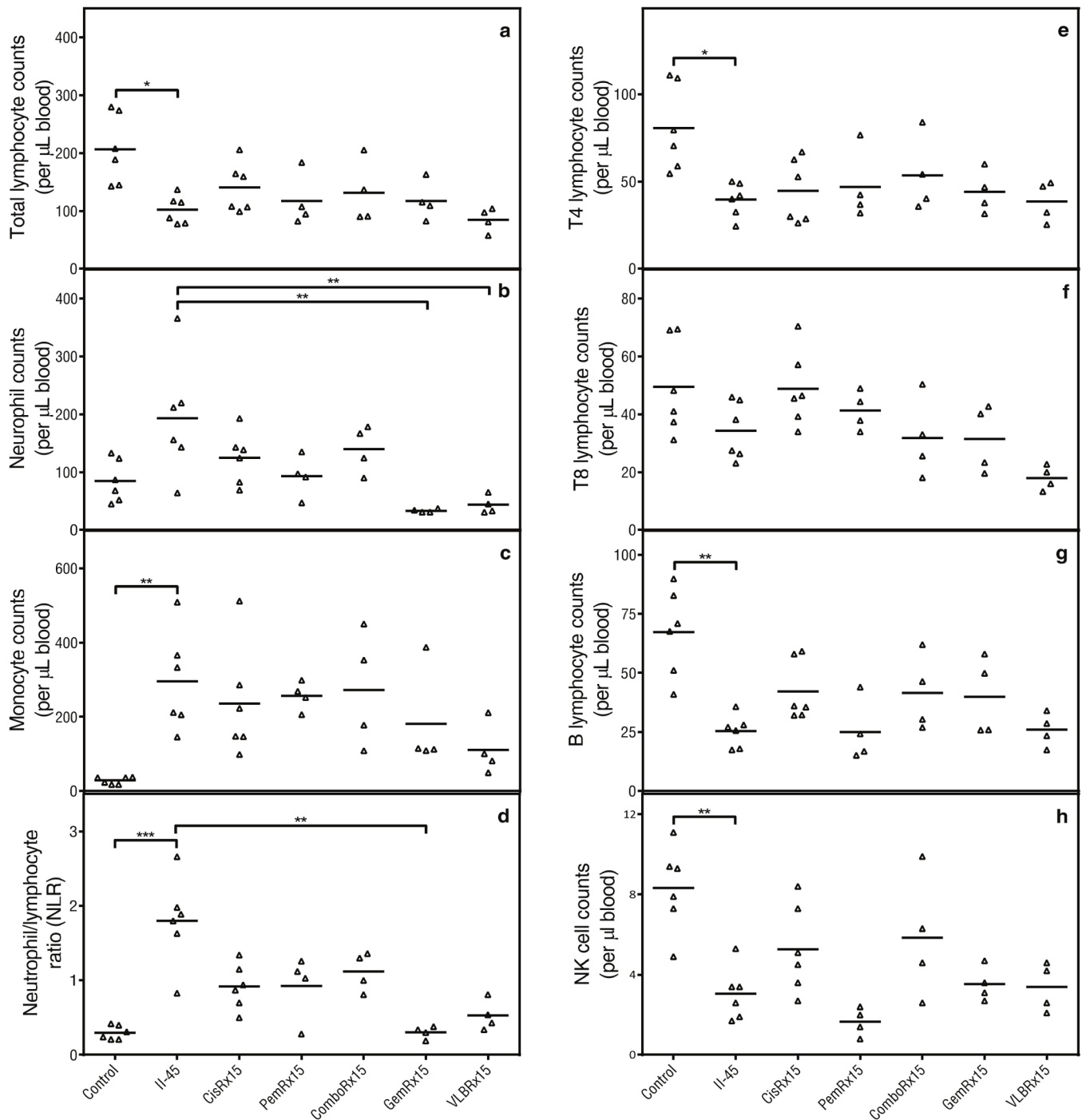


**Figure 5 | Total white blood cell counts.** Rats were injected with 100  $\mu\text{L}$  serum free media or serum free media containing  $5 \times 10^5$  parental or chemo-resistant II-45 cells directly into the pleural cavity. At ethical endpoint, rats were euthanized and whole blood samples were analysed relative to rats with parental II-45 mesothelioma. (a) total lymphocyte counts; (b) total neutrophil counts; (c) total monocyte counts; (d) neutrophil to lymphocyte ratio (NLR); (e) CD4 positive (T4) lymphocyte counts; (f) CD8 positive (T8) lymphocyte counts; (g) CD45 RA positive B lymphocyte counts; (h) total number of peripheral natural killer (NK) cells. Normal control rats, Control; parental mesothelioma cells, II-45; cisplatin resistant II-45 cells, CisR; pemetrexed resistant II-45 cells, PemR; combination (cisplatin + pemetrexed) resistant II-45 cells, ComboR; gemcitabine resistant II-45 cells, GemR; vinorelbine resistant II-45 cells, VLBR. P-values were calculated using a one-way Anova test with a value of less than 0.05 indicating significance. \* $p < 0.05$ , \*\* $p < 0.01$ , \*\*\* $p < 0.001$  relative to rats with parental II-45 mesothelioma.

carcinoma-related markers TTF-1 and CD15 (data not shown). Equivalent patterns and intensity were noted for tumors arising from both parental and chemo-resistant cells for the positive markers WT-1, HBME-1, calretinin and both cytokeratins with representative images shown in supplementary Figure 5. However, while podoplanin was also positive in all tumors, increased expression was

observed in the tumors derived from PemR cells (Figures 4B & 4C) confirming the predominantly sarcomatoid morphology observed for these tumours (Figure 4A).

**Circulating immune cell profiling and cytokine analysis identifies generalised immune suppression in rats with mesothelioma.** In

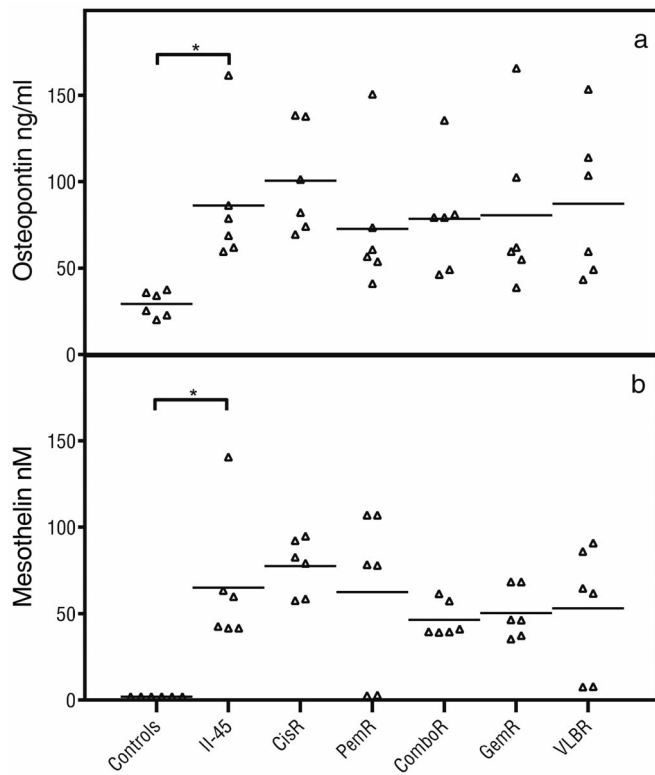


**Figure 6 | Plasma endpoint biomarkers.** Rats were injected with 100  $\mu$ L serum free media or serum free media containing  $5 \times 10^5$  parental or chemo-resistant II-45 cells directly into the pleural cavity. At ethical endpoint, rats were euthanized and plasma samples were analysed for cytokine levels relative to rats with parental II-45 mesothelioma. (a) osteopontin levels; (b) mesothelin levels. Normal control rats, Control; parental mesothelioma cells, II-45; cisplatin resistant II-45 cells, CisR; pemetrexed resistant II-45 cells, PemR; combination (cisplatin + pemetrexed) resistant II-45 cells, ComboR; gemcitabine resistant II-45 cells, GemR; vinorelbine resistant II-45 cells, VLBR. P-values were calculated using a one-way Anova test with a value of less than 0.05 indicating significance. \* $p < 0.05$  relative to rats with parental II-45 mesothelioma.

human MM, the immune system plays a key role in tumorigenesis and tumour maintenance with chronic inflammation preceding the development of malignancy and MM cells having the ability to evade surveillance by the immune system and contribute to systemic changes. In our models tumor initiation is by engraftment and thus tumorigenesis cannot be assessed. However, we were interested to determine whether the established tumor was able to alter the host's immune response in a similar way as mesothelioma does in humans. To assess the systemic effects of the tumors, circulating immune cells and cytokines were profiled. Peripheral blood samples from rats with parental pleural II-45 cells were firstly evaluated in relation to normal healthy control rats (Figure 5). Total lymphocyte counts as well as the individual subsets (CD4, B cells and NK cells) were significantly decreased ( $p \leq 0.05$ ) while total monocyte counts as well as the neutrophil to lymphocyte ratio (NLR) were significantly elevated ( $p < 0.01$ ). Significantly elevated levels of osteopontin ( $p < 0.05$ ) and mesothelin ( $p < 0.05$ ) were also identified in rats with parental II-45 cells in relation to control rats (Figure 6). Down regulation of both pro- and anti-inflammatory cytokines was also identified in the serum of animals with mesothelioma (supplementary Figure 6). These results suggest an overall immune suppression in rats with MM.

Additionally, to determine whether drug pre-treatment of mesothelioma cells influences the host's immune response, we also directly compared rats with parental II-45 cells to rats with chemo-resistant II-45 cells. Total neutrophil counts were significantly decreased in rats with gemcitabine resistant and vinorelbine resistant II-45 cells ( $p < 0.01$ ) while NLR was significantly decreased only in rats with gemcitabine resistant II-45 cells ( $p < 0.01$ ). Interestingly, increased levels of IL-7 and GM-CSF were identified in rats with vinorelbine resistant II-45 cells and increased levels of GRO/KC was identified in rats with cisplatin resistant cells ( $p < 0.05$ ; supplementary Figure 6).

## Discussion

This paper establishes and characterizes a panel of chemo-resistant models for mesothelioma research which have clinically relevant levels of resistance. We have used a standard pulsed treatment strategy followed by recovery in drug free media in order to mimic the cycles of chemotherapy a cancer patient receives in the clinic. While the acquired resistance levels that developed in our cells are relatively low, similar levels are found in cell lines derived from cancer patient's pre and post chemotherapy suggesting our models have clinically relevant levels of resistance (reviewed<sup>26</sup>). In addition to our models developing clinically relevant levels of chemo-resistance, they were also found to contain similar gene changes and chromosomal abnormalities as those found in human mesothelioma samples with increased expression of many ABC transporter proteins<sup>27,28,36</sup> and homozygous deletion of the p16<sup>INK4A</sup>/p14<sup>ARF</sup> locus<sup>34</sup>, thus highlighting the biological and clinical relevance of our models to the human malignancy.

The results from our study highlight the contribution the drug transport or efflux pumps have on chemo-resistance in our models. While inhibitors of these proteins exists, the use of these in the clinical setting has resulted in limited success (reviewed in<sup>37</sup>) primarily due to chemo-resistance being a multifactorial complex problem. Other known mechanisms such as increased expression of *Ercc1*<sup>29</sup>, *Rrm1*<sup>30</sup> and *Tyms*<sup>31</sup> were shown to be of lower importance in our models however future studies comprehensively examining these mechanisms will help shed light on this overarching issue.

Given that tumor morphology is an important indicator of prognosis in the human disease, with sarcomatoid morphology indicating reduced survival and reduced responsiveness to treatment<sup>21</sup>, it was intriguing to note that the acquisition of chemo-resistance *in vitro* resulted in morphological changes *in vivo*. For tumors derived from PemR cells, this sarcomatoid morphology was corroborated by increased podoplanin expression, a immuno-marker considered especially useful for sarcomatoid MM diagnosis<sup>38</sup>. In addition, this increased podoplanin expression also corresponded with decreased survival in PemR animals which correlates with a recent finding by Yamaki *et al.*<sup>39</sup> who suggested high expression of podoplanin as a prognostic marker of decreased survival in human mesothelioma. While not previously reported in MM, this change in morphology has been reported in colorectal cancer using similarly matched parental and chemo-resistant cell lines<sup>40</sup>. Post-chemotherapy biopsy of MM patients is not part of the standard of care and therefore it is unknown whether such morphological changes resulting from acquired chemo-resistance also occur in MM patients and whether this change is associated with reduced survival. Thus pre-clinical models of MM with differences in acquired resistance and morphology that recapitulate those seen in the human malignancy may provide insights for the choice of efficacious 2<sup>nd</sup> line therapies not possible using human samples.

Using a syngeneic cell line as the platform for the generation of chemo-resistant cells has several advantages over the traditional xenograft models. These models overcome the problems of incompatibility of the tumor cell and host, and the immunodeficiency of the host which has allowed us to create a more realistic environment for





tumor development and, for eventual drug testing<sup>14</sup>. Assessing the immune systems of our animals has again helped confirmed the relevance of our models to the human malignancy, but has also highlighted that the acquisition of chemo-resistance can alter the host's immune response. While the reason for these differences requires further investigation, *in vitro* drug pre-treatment of cells has been previously documented to alter the immune response when grown *in vivo*<sup>41,42</sup>. These results also support previous studies where changes in immune biomarker levels have been found to correspond with the development of chemo-resistance<sup>43</sup>, and, as such may be predictive of such occurrences<sup>44,45</sup>. The acquisition of resistance therefore may be one of the reasons why immune biomarker levels in human mesothelioma patients are more varied and why they are not yet approved for clinical use.

In conclusion, having characterized these cell lines at multiple levels and identified similarities with the human malignancy, the models generated will enable rapid screening of novel single agent or combination therapies for evidence of cytotoxic activity in the setting of chemo-resistance. This will inform further pre-clinical and planned clinical development of these agents, thus providing a valuable new resource for initial drug screening to help address a major unmet need in the care of patients with mesothelioma.

## Methods

**Animal studies.** All procedures involving animals were carried out in accordance with the recommendations in the Australian Code of Practice for the Care and Use of Animals for Scientific Purposes. The protocol for this study was approved by the Royal North Shore Hospital Animal Care and Ethics Committee (protocol numbers 1110-018A and 1206-013A).

Female Fischer 344 rats weighing 150–200 g were maintained at the Kearns Facility under standard conditions (12 hrs. light/dark cycles and free access to food and water).

**Cell lines.** The syngeneic rat mesothelioma II-45 cell line<sup>15</sup> was a kind gift from A/Prof. Emanuela Felley-Bosco, Zurich University. The normal mesothelial 4/4 RM.4 cell line from female Fischer 344 rats was purchased from the ATCC (CCL-216). Cells were cultured and maintained in RPMI 1640 supplemented with 10% fetal bovine serum and grown in standard conditions (37°C humidified incubator with 5% CO<sub>2</sub>).

**Cytotoxicity assays.** Assays were performed in triplicate in a final volume of 200 μL. 4 × 10<sup>3</sup> cells in 100 μL were plated into 96-well microtitre plates and left to adhere for approximately 4 hrs. Serial drug dilutions (100 μL) were then added and plates were incubated for 72 hrs. in standard cell culture conditions. For experiments utilizing verapamil or buthionine sulfoximine (BSO), a final concentration of 20 μM and 50 μM (respectively) was also added to the cells. The MTT (3-(4,5-dimethylthiazol-2-yl)-2,5-diphenyl tetrazolium bromide) assay was performed as previously described to determine cell viability<sup>46</sup> and to establish the drug dose causing 50% growth inhibition (IC<sub>50</sub> drug dose). GraphPad Prism non-linear (curve fit) regression algorithms were used to calculate the drug dose causing 50% growth inhibition (IC<sub>50</sub> drug dose).

**Generation of chemo-resistant cell lines.** II-45 cells were exposed to the IC<sub>50</sub> drug dose of standard chemotherapies (as determined above) for 72 hrs. Drug was then removed and cells were allowed to recover. Upon recovery, cells were again treated with the same concentration of chemotherapy for 72 hrs. Drug was again removed and cells were allowed to recover. This process was repeated a total of 15 times in order to generate clinically relevant chemo-resistant cell lines; IC<sub>50</sub> drug dose used: cisplatin (0.3 μg/ml), pemetrexed (25 ng/ml), combination of cisplatin + pemetrexed (0.3 μg/ml cisplatin + 25 ng/ml pemetrexed), gemcitabine (2 ng/ml) and vinorelbine (16 nM).

**Tumor induction and analysis.** A total of 100 μL of serum free media or serum free media containing 5 × 10<sup>5</sup> parental or chemo-resistant II-45 cells was injected into the pleural cavity of female Fischer rats (n ≥ 4 for each group) approximately 0.5 cm proximal to the 2<sup>nd</sup> nipple. Rats were euthanized at ethically approved endpoints (weight loss of >10% or difficulty in breathing) and samples collected. Tumors were scored on a scale of 1 to 5 based on volume and infiltration of tumor into the pleural cavity; 1 indicating the tumor occupied up to 10% of the pleural cavity and 5 indicating the tumor occupied 40–50% of the pleural cavity. Tumors were fixed for histopathological examination or immediately frozen in liquid nitrogen and stored at –80°C for gene expression analysis.

**In vivo engraftment with chemotherapy treatment.** A total of 100 μL of serum free media containing 1 × 10<sup>6</sup> parental or CisR II-45 cells was injected sub-dermally into the flank of female Fischer rats (n = 2 for each group). On day 3 rats received 2 mg/kg cisplatin intraperitoneally as well as 5 ml saline subcutaneously at the neck. This was

repeated on days 14, 21 and 36 (a total of 4 doses). Tumors were measured by calipers (on the same days as dosing) and tumor volume was calculated using the equation (width<sup>2</sup>/length)/2 = cm<sup>3</sup>. Rats were euthanized at ethically approved endpoints (tumor size > 13.5 cm<sup>3</sup> or weight loss of >10%) and samples collected. *Ex-vivo* transplants were taken and cultured in standard conditions in the presence of antibiotics (penicillin/streptomycin) and their resistance profiles assessed following the cytotoxicity assays method above.

**Histological analyses.** Histopathological analysis was performed to confirm and characterize the subtype of mesothelioma. Following euthanasia, pleural tumors (n ≥ 3) were excised immediately and tumor pieces approximately 3 mm thick were fixed in 4% paraformaldehyde overnight at 4°C, then processed and embedded in paraffin. Sections cut 5 μm thick were stained with haematoxylin and eosin (H&E).

**Immunohistological analyses.** A panel of antibodies commonly used to establish a pathologic diagnosis of mesothelioma was used to characterize rat tumors<sup>5,38,47,48</sup>. Supplementary table 1 lists the primary antibodies and the optimized conditions for each antibody. Of note, the selection of antibodies recognizing rat antigens is limited and many antibodies used for human studies are not available for rat tissue<sup>49</sup>. Antigen retrieval was performed in 10 mM Tris/1 mM EDTA pH 9 (with the exception of the Ki67 antibody which was performed in 10 mM citrate buffer pH6) by immersion in a boiling water bath for 20 minutes except for HBME-1 (no retrieval necessary). This was followed by an endogenous peroxidase block using 0.3% H<sub>2</sub>O<sub>2</sub> for 10 minutes. Overnight incubation at 4°C in a Sequenza rack was performed for all primary antibodies. Mouse/rabbit Envision+ was used routinely for detection, followed by 3,3'-Diaminobenzidine (DAB) according to the manufacturer's recommendations. Positive and negative control tissues and isotype reagent controls were included.

**Blood and plasma. Blood analysis.** A four-color flow cytometry assay was developed using the FACS Calibur Flow cytometer (Becton Dickinson and Company (BD), North Ryde, New South Wales, Australia) and a panel of antibodies (supplementary table 2) to examine changes in leukocyte cell counts as a result of mesothelioma. At endpoint, blood from each rat group (n ≥ 4) was collected in EDTA tubes for immediate analysis. A small sample of EDTA-whole blood (25 μL) was added to True Count tubes (BD) together with 10 μL of anti-rat CD4-FITC, anti-rat CD8a-PE and anti-rat CD45-PE/Cy7 and 20 μL of rat T/B/NK cocktail. Samples were incubated for 15 minutes at room temperature and then lysed using 10 mM Tris and ammonium chloride buffer (pH 7.5). Multiple cell populations were analysed; CD4 positive cells were identified as CD45<sup>+</sup>/CD3<sup>+</sup>/CD4<sup>+</sup>, CD8 positive cells were identified as CD45<sup>+</sup>/CD3<sup>+</sup>/CD8<sup>+</sup>, Natural Killer (NK) cells were identified as CD45<sup>+</sup>/CD3<sup>-</sup>/CD161a<sup>+</sup> and B cells were identified as CD45<sup>+</sup>/CD3<sup>-</sup>/CD45RA<sup>+</sup>. Absolute numbers of leukocytes (per μL) were determined using the ratio between cellular events and fluorescent bead events using the formula (cell count/25 μL) × (bead count/bead value defined by the manufacturer).

**Plasma analysis.** Rat EDTA-plasma samples (n ≥ 3 for each group) were analyzed for cytokine levels using the Rat Cytokine 23-plex (Biorad, Gladesville, New South Wales, Australia) following the manufacturer's instructions. Plasma levels for mesothelin and osteopontin were determined using the rat N-ERC/mesothelin (Immuno-Biological Laboratories, Gunma, Japan) and the rat osteopontin (USCN Life Sciences, Houston, Texas, USA) ELISA kits respectively.

**Quantitative real time PCR.** RNA from snap frozen rat tumors or cells within linear phase was extracted using Trizol and then purified using the RNeasy mini kit according to each manufacturer's instructions.

**Drug resistance and metabolism quantitative real time PCR arrays.** Following quality analysis and quantification, RNA was reverse transcribed using the RT cDNA synthesis first strand synthesis kit. Quantitative real time PCR was performed using SYBR green and the SABiosciences Drug Resistance and Metabolism PCR Arrays on the Applied Biosystems 7900HT real time PCR system according to the manufacturer's instructions. Three biological replicates were performed for each cell line and tumor sample, and the results were analyzed using the SABiosciences PCR Array Data Analysis Software. Fold changes in each individual gene expression were calculated independently using the 2<sup>-delta-delta Ct</sup> method after normalizing to a panel of housekeeping genes (*Rplp1*, *Hprt1*, *Rpl13a*, *Ldha* and *Actb*).

**TaqMan gene expression assays.** Individual TaqMan gene expression assays were used to validate selected genes from the PCR array or to investigate genes correlated with chemo-resistance according to the manufacturer's instructions. Three biological replicates were performed for each cell line and tumor sample, and the results were analyzed using the Data Assist Software v3.0. Fold changes in each individual gene expression were calculated independently using the 2<sup>-delta-delta Ct</sup> method after normalizing to a panel of housekeeping genes (*Rplp1*, *Actb* and *Gapdh*).

**Comparative genomic hybridization arrays.** Four biological replicates of the parental and combination resistant (cisplatin + pemetrexed) II-45 cell lines were harvested during log phase and DNA was extracted using the DNeasy blood and tissue kit (Qiagen) according to the manufacturer's instructions. Following quality analysis and quantification, comparative genomic hybridization (CGH) was commercially performed for each DNA sample using 4 × 180 K format custom made rat Agilent CGH arrays by the Ramaciotti Gene Analysis Centre, Randwick, NSW,



Australia. Additional probes were added to the standard format to increase coverage for genes of interest (*Cdkn2a/b*, *Nf2*, *Tp53*, *Bap1* and *Egfr*). Arrays were normalized using diploid peak (default settings) and aberrations were calculated using the ADM-1 algorithm of the Agilent Genomic Workbench v7 program. For each array, the 4/4 RM.4 cell line was used as a reference and labelled with Cy-3. Samples of interest were labelled with Cy-5.

**Statistical analysis.** The statistical analysis package GraphPad Prism (v4) was used to perform t-tests, one-way Anova tests or log-rank (Mantel-Cox) Gehan-Breslow-Wilcoxon survival tests, with a p-value of less than 0.05 indicating significance.

- WHO. Asbestos: elimination of asbestos-related diseases. *Fact sheet No 343*, July, 2010.
- Sim, M. R. A worldwide ban on asbestos production and use: some recent progress, but more still to be done. *Occup Environ Med* **70**, 1–2 (2013).
- Olsen, N. J. *et al.* Increasing incidence of malignant mesothelioma after exposure to asbestos during home maintenance and renovation. *Med J Aust* **195**, 271–274 (2011).
- Vogelzang, N. J. *et al.* Phase III study of pemetrexed in combination with cisplatin versus cisplatin alone in patients with malignant pleural mesothelioma. *J Clin Oncol* **21**, 2636–2644 (2003).
- Guidelines for the diagnosis and treatment of malignant pleural mesothelioma. *The Asbestos Diseases Research Institute Place* published (2013).
- Remon, J. *et al.* Malignant mesothelioma: New insights into a rare disease. *Cancer Treat Rev* (2012).
- Zucali, P. A. *et al.* Advances in the biology of malignant pleural mesothelioma. *Cancer Treat Rev* **37**, 543–558 (2011).
- Zauderer, M. G. & Krug, L. M. Novel therapies in phase II and III trials for malignant pleural mesothelioma. *J Natl Compr Canc Netw* **10**, 42–47 (2012).
- Yakisich, J. S. An Algorithm for the Preclinical Screening of Anticancer Drugs Effective against Brain Tumors. *ISRN Pharmacol* **2012**, 513580 (2012).
- Kamb, A. What's wrong with our cancer models? *Nat Rev Drug Discov* **4**, 161–165 (2005).
- Lowenstein, P. R. & Castro, M. G. Uncertainty in the translation of preclinical experiments to clinical trials. Why do most phase III clinical trials fail? *Curr Gene Ther* **9**, 368–374 (2009).
- Favoni, R. E., Daga, A., Malatesta, P. & Florio, T. Preclinical studies identify novel targeted pharmacological strategies for treatment of human malignant pleural mesothelioma. *Br J Pharmacol* **166**, 532–553 (2012).
- Frese, K. K. & Tuveson, D. A. Maximizing mouse cancer models. *Nat Rev Cancer* **7**, 645–658 (2007).
- Abolhassani, M. *et al.* Screening of well-established drugs targeting cancer metabolism: reproducibility of the efficacy of a highly effective drug combination in mice. *Invest New Drugs* (2011).
- Craighead, J. E., Akley, N. J., Gould, L. B. & Libbus, B. L. Characteristics of tumors and tumor cells cultured from experimental asbestos-induced mesotheliomas in rats. *Am J Pathol* **129**, 448–462 (1987).
- Shi, Y. *et al.* Bioluminescence imaging for in vivo monitoring of local recurrence mesothelioma model. *Lung Cancer* **71**, 370–371 (2011).
- Kucharczuk, J. C. *et al.* Pleural-based mesothelioma in immune competent rats: a model to study adenoviral gene transfer. *Ann Thorac Surg* **60**, 593–597; discussion 597–598 (1995).
- Lardinois, D. *et al.* Intrapleural topical application of cisplatin with the surgical carrier Vivostat increases the local drug concentration in an immune-competent rat model with malignant pleuromesothelioma. *J Thorac Cardiovasc Surg* **131**, 697–703 (2006).
- Opitz, I. *et al.* Local recurrence model of malignant pleural mesothelioma for investigation of intrapleural treatment. *Eur J Cardiothorac Surg* **31**, 773–778 (2007).
- Zhong, J., Lardinois, D., Szilard, J., Tamm, M. & Roth, M. Rat mesothelioma cell proliferation requires p38delta mitogen activated protein kinase and C/EBP-alpha. *Lung Cancer* (2011).
- Nutt, J. E. *et al.* The role of folate receptor alpha (FRalpha) in the response of malignant pleural mesothelioma to pemetrexed-containing chemotherapy. *Br J Cancer* **102**, 553–560 (2010).
- Kao, S. C. *et al.* Validation of prognostic factors in malignant pleural mesothelioma: a retrospective analysis of data from patients seeking compensation from the New South Wales dust diseases board. *Clin Lung Cancer* **14**, 70–77 (2013).
- Aronson, J. F. & Cristofalo, V. J. Culture of epithelial cells from the rat pleura. *In Vitro* **17**, 61–70 (1981).
- Bermudez, E., Libbus, B. & Mangum, J. B. Rat pleural mesothelial cells adapted to serum-free medium as a model for the study of growth factor effects. *Cell Biol Toxicol* **14**, 243–251 (1998).
- Swain, W. A., O'Byrne, K. J. & Faux, S. P. Activation of p38 MAP kinase by asbestos in rat mesothelial cells is mediated by oxidative stress. *Am J Physiol Lung Cell Mol Physiol* **286**, L859–865 (2004).
- McDermott, M. *et al.* In vitro Development of Chemotherapy and Targeted Therapy Drug-Resistant Cancer Cell Lines: A Practical Guide with Case Studies. *Front Oncol* **4**, 40 (2014).
- Shukla, A. *et al.* Blocking of ERK1 and ERK2 sensitizes human mesothelioma cells to doxorubicin. *Mol Cancer* **9**, 314 (2010).
- Goparaju, C. M. *et al.* Oncogene mediated NFKbeta downregulation in malignant pleural mesothelioma. *Oncogene* **30**, 2767–2777 (2011).
- Dabholkar, M., Vionnet, J., Bostick-Bruton, F., Yu, J. J. & Reed, E. Messenger RNA levels of XPAC and ERCC1 in ovarian cancer tissue correlate with response to platinum-based chemotherapy. *J Clin Invest* **94**, 703–708 (1994).
- Davidson, J. D. *et al.* An increase in the expression of ribonucleotide reductase large subunit 1 is associated with gemcitabine resistance in non-small cell lung cancer cell lines. *Cancer Res* **64**, 3761–3766 (2004).
- Obata, T., Tanaka, M., Suzuki, Y. & Sasaki, T. The Role of Thymidylate Synthase in Pemetrexed-Resistant Malignant Pleural Mesothelioma Cells. *Journal of Cancer Therapy* **4**, 1052–1059 (2013).
- Kruh, G. D. & Belinsky, M. G. The MRP family of drug efflux pumps. *Oncogene* **22**, 7537–7552 (2003).
- Kartalou, M. & Essigmann, J. M. Mechanisms of resistance to cisplatin. *Mutat Res* **478**, 23–43 (2001).
- Jean, D., Daubriac, J., Le Pimpec-Barthes, F., Galateau-Salle, F. & Jaurand, M. C. Molecular changes in mesothelioma with an impact on prognosis and treatment. *Arch Pathol Lab Med* **136**, 277–293 (2012).
- Iwanami, T. *et al.* Clinical significance of epithelial-mesenchymal transition-associated markers in malignant pleural mesothelioma. *Oncology* **86**, 109–116 (2014).
- Soini, Y., Jarvinen, K., Kaarteenaho-Wiik, R. & Kinnula, V. The expression of P-glycoprotein and multidrug resistance proteins 1 and 2 (MRP1 and MRP2) in human malignant mesothelioma. *Ann Oncol* **12**, 1239–1245 (2001).
- Shukla, S., Ohnuma, S. & Ambudkar, S. V. Improving cancer chemotherapy with modulators of ABC drug transporters. *Curr Drug Targets* **12**, 621–630 (2011).
- Chirieac, L. R. *et al.* The immunohistochemical characterization of sarcomatoid malignant mesothelioma of the pleura. *Am J Cancer Res* **1**, 14–24 (2011).
- Yamaki, E. *et al.* Podoplanin overexpression in human mesothelioma cell lines enhances the tumorigenic phenotype. *Oncol Rep* **29**, 932–940 (2013).
- Dallas, N. A. *et al.* Chemoresistant colorectal cancer cells, the cancer stem cell phenotype, and increased sensitivity to insulin-like growth factor-I receptor inhibition. *Cancer Res* **69**, 1951–1957 (2009).
- Guillot, F. *et al.* Vaccination with epigenetically treated mesothelioma cells induces immunisation and blocks tumour growth. *Vaccine* (2011).
- Thomas-Schoemann, A. *et al.* Bystander effect of vinorelbine alters antitumor immune response. *Int J Cancer* **129**, 1511–1518 (2011).
- Hodgkinson, V. C. *et al.* Proteomic identification of predictive biomarkers of resistance to neoadjuvant chemotherapy in luminal breast cancer: a possible role for 14-3-3 theta/tau and tBID? *J Proteomics* **75**, 1276–1283 (2012).
- Kitayama, J., Yasuda, K., Kawai, K., Sunami, E. & Nagawa, H. Circulating lymphocyte is an important determinant of the effectiveness of preoperative radiotherapy in advanced rectal cancer. *BMC Cancer* **11**, 64 (2011).
- Lissoni, P. *et al.* Efficacy of cancer chemotherapy in relation to the pretreatment number of lymphocytes in patients with metastatic solid tumors. *Int J Biol Markers* **19**, 135–140 (2004).
- Mosmann, T. Rapid colorimetric assay for cellular growth and survival: application to proliferation and cytotoxicity assays. *J Immunol Methods* **65**, 55–63 (1983).
- Kao, S. C. *et al.* Validation of a minimal panel of antibodies for the diagnosis of malignant pleural mesothelioma. *Pathology* **43**, 313–317 (2011).
- Ordóñez, N. G. What are the current best immunohistochemical markers for the diagnosis of epithelioid mesothelioma? A review and update. *Hum Pathol* **38**, 1–16 (2007).
- Hu, Q. *et al.* Homozygous deletion of CDKN2A/2B is a hallmark of iron-induced high-grade rat mesothelioma. *Lab Invest* **90**, 360–373 (2010).

## Acknowledgments

We would like to thank A/Prof. Emanuela Felley-Bosco from Zurich University for kindly providing us with the II-45 cell line.

## Author contributions

A.L.H. and C.W. conceived and designed the experiments. A.H., C.W., E.M. and R.H. performed the experiments. A.L.H., C.W., E.M. and S.K. analyzed the data. S.K., S.J.C., N.P. and V.M.H. advised on the research and conceived the project. All authors reviewed and revised the manuscript.

## Additional information

**Supplementary information** accompanies this paper at <http://www.nature.com/scientificreports>

**Competing financial interests:** The authors declare no competing financial interests.

**How to cite this article:** Hudson, A.L. *et al.* Establishing a panel of chemo-resistant mesothelioma models for investigating chemo-resistance and identifying new treatments for mesothelioma. *Sci. Rep.* **4**, 6152; DOI:10.1038/srep06152 (2014).



This work is licensed under a Creative Commons Attribution-NonCommercial-NoDerivs 4.0 International License. The images or other third party material in this article are included in the article's Creative Commons license, unless indicated otherwise in the credit line; if the material is not included under the Creative

Commons license, users will need to obtain permission from the license holder in order to reproduce the material. To view a copy of this license, visit <http://creativecommons.org/licenses/by-nc-nd/4.0/>